A LONG-RANGE COMPUTATIONAL RFID TAG FOR TEMPERATURE AND ACCELERATION SENSING APPLICATIONS

Danilo De Donno[*], Luca Catarinucci, Adolfo Di Serio, and Luciano Tarricone

Department of Innovation Engineering, University of Salento, Via Monteroni, Lecce 73100, Italy

Abstract—In this paper, the design, realization, and experimental validation of a battery-assisted radio frequency identification (RFID) tag featuring sensing and computation capabilities are presented. The sensor-augmented RFID tag comprises an ultra-low-power microcontroller, temperature sensor, 3-axis accelerometer, non-volatile storage, and a new-generation I^{2}C-RFID chip for communication with standard UHF EPCglobal Class-1 Generation-2 readers. A preliminary printed-circuit-board prototype, connected to a 3-V/225-mAh lithium battery, provides a lifetime up to approximately 3 years when sensing and RFID-based communication tasks are performed every 10 seconds. Moreover, the device exhibits indoor transmission ranges up to 22 m, 6 m, and 5 m when attached to foam, concrete, and wood respectively. The encouraging results achieved for an emulated application scenario demonstrate the suitability of the device to be adopted in contexts where temperature and acceleration sensing are required.

1. INTRODUCTION

Sensor-enabled radio frequency identification (RFID) tags are becoming increasingly popular because of their ability to add value over conventional identification-only tags in a variety of application scenarios. For example, monitoring of transport parameters (e.g., temperature threshold violations in perishable goods or unsafe accelerations experienced by fragile items), besides being crucial to ensure the delivery of high-quality products, is legally required by

European regulations. Other applications of sensor-enabled RFID tags include disaster prevention and recovery, surveillance, home automation [1], healthcare [2], structure and machine diagnosis.

In the last few years, the integration of communication, computation, sensing, and storage functionalities in ultra-high-frequency (UHF) RFID tags — operating frequencies 865–868 MHz in Europe, 902–928 MHz in North America and Japan — has raised widespread interest among researchers, practitioners, and industrial enterprises. The pioneers in conceiving *augmented* UHF RFID tags were Smith et al. in 2008 with their wireless identification and sensing platform (WISP) [3], which is a battery-free programmable tag with sensors supporting, however, only a limited number of commands and functionalities of the EPC Class-1 Generation-2 (Gen2 for short hereafter) protocol. In our earlier work [4], we present a short-range passive UHF RFID tag for temperature-sensing applications fully compliant with the Gen2 standard. A battery-assisted Gen2-compliant RFID tag integrating a moisture sensor, occupying an area of $15 \times 11 \, \text{cm}^2$, and achieving a maximum read range of 3.4 m is presented in [5]. Finally, authors of [6] discuss the implementation of a battery-assisted UHF RFID tag prototype with an on-board digital temperature sensor. The tag is compatible with the Gen2 protocol, is programmable, and exhibits a maximum operating range of 12 m.

In addition to the research activity, RFID manufacturers have recently broken into the market with Gen2 tags integrating sensing, computation, and data-logging capabilities for *unconventional* RFID applications. Among them, it is worth mentioning the SL900A sensory tag by Austria Micro Systems (AMS), the Easy2Log tag by CAEN RFID, and the SensTAG by Phase IV. Nevertheless, none of the aforementioned solutions integrates all the primary characteristics required for future RFID-based sensing applications, e.g., the full compliance with RFID standards and regulations (most devices need specific settings for the reader), a satisfactory operating range, a variety of on-board sensors, high expansibility and programmability. Note that *active* tags are not considered in this work since, in most cases, proprietary protocols with no interoperability among manufacturers are used for this class of tags.

This work presents the design, prototyping, and experimental validation of a long-range, Gen2-compliant, and programmable RFID tag with on-board sensors (referred to in the sequel as sensor-augmented RFID tag) enabling RFID-based sensing applications beyond the mere object identification. The device relies on the exploitation of a novel RFID chip with dual communication interface: a wired I^2C interface managed by a microcontroller and a wireless UHF
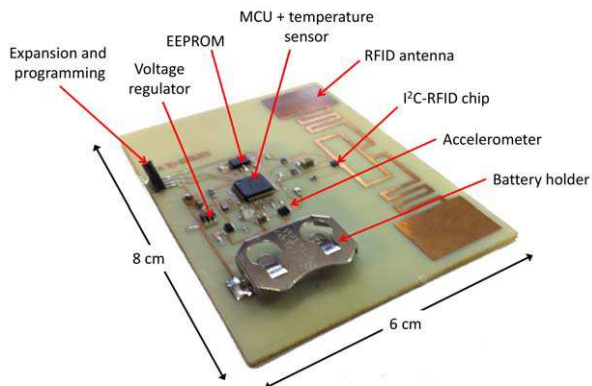
Figure 1. Prototype of the developed sensor-augmented RFID tag.

interface for communication with standard Gen2 readers. The sensor-augmented RFID tag operates in battery-assisted-passive (BAP) mode, i.e., it communicates with the reader via the zero-power backscattering technique but derives power from an on-board battery. The device is fabricated using off-the-shelf low-cost discrete components on an FR4 substrate (see Fig. 1) and is equipped with microcontroller unit (MCU), temperature sensor, 3-axis accelerometer, and a large EEPROM for data logging. As discussed later in the paper, the sensor-augmented RFID tag exhibits appealing performance in terms of power consumption and maximum communication distance with the reader, even when mounted on harsh, rugged surfaces. Moreover, in contrast to application-specific fixed-function IC products, our approach, based on a printed-circuit-board open-hardware design, offers flexibility to interface new sensors, actuators, modules, and devices for further expanding the range of applications, e.g., towards heterogeneous Wireless Sensor Networks (WSN) [7]. A real-world experiment illustrative of the capabilities provided by the sensor-augmented RFID tag is presented at the end of the paper: the device is used to monitor ambient temperature conditions and static acceleration of a parcel in order to catch significant events (e.g., displacements, abusive handling, temperature threshold violations, etc.) during a simulated shipment.

This paper is organized as follows. Architecture, components, and design of the sensor-augmented RFID tag are discussed in Section 2. A series of experiments aimed at assessing the device performance are presented in Section 3 along with a potential use-case scenario concerning temperature and acceleration monitoring. Finally, conclusions are drawn in Section 4.

2. DESIGN AND IMPLEMENTATION

The design here proposed for the sensor-augmented RFID tag relies on a simple yet effective operating principle. A canonical UHF RFID tag, composed of a dipole-like antenna and a Gen2 chip, makes up the radio front end. The main peculiarity of the adopted RFID chip is the capability of its memory to be accessed via the wired I^{2}C interface, in addition to the standard Gen2 wireless interface. As a consequence, sensor data transferred over the I^{2}C bus by means of an MCU are directly accessible to conventional RFID Gen2 readers.

The sensor-augmented RFID tag is powered by a 3-V/225-mAh CR2032 button-cell lithium battery connected to a TI TPS78330 3-V low-dropout (LDO) linear voltage regulator. Additional energy sources or energy-harvesting modules [8, 9] can be easily interfaced with the device by connecting them directly to the LDO regulator. The core of the system is an ultra-low-power 16-bit MSP430F5310 MCU which can run up to 25 MHz with 3-V supply voltage and consumes approximately 115 μA/MHz. The supply current reduces to 1.9 μA/MHz in sleep mode with real-time clock crystal, full RAM retention, and 5-μs wake-up time. The MCU provides also 32 kB of flash memory, 6 kB of SRAM, a 12-channel 10-bit 200-ksps Analog-to-Digital Converter (ADC), and 47 GPIO. To further extend the storage capabilities of the device, an additional 256-kB serial CMOS EEPROM is interfaced with the MCU via the I^{2}C bus.

The MCU is programmed with an energy-efficient firmware running at 1 MHz and implementing I^{2}C read/write and ADC sampling routines. The 10-bit ADC samples the integrated analog temperature sensor consuming down to 9 μA. Then, readings from an ADXL346 accelerometer are taken via the I^{2}C interface. The ADXL346 is an ultra-low power (23-μA current consumption) 3-axis accelerometer with 13-bit resolution measurements for each axis up to ±16 g. The sensor readings are wrapped in a 64-bit data chunk — 10-bit temperature, 13-bit acceleration for each of the three axes, and 15-bit read counter — which is written (via the I^{2}C bus) into the password-protected *user memory* of the RFID Gen2 chip. Such an approach leaves the 96-bit EPC of the tag totally reserved for device/product identification, thus enabling fully EPCglobal-compliant applications.

A compact dipole-like RFID antenna has been designed for the radio front end. The complex input impedance of the antenna has been tuned to match that of an Impinj Monza X-2K RFID chip ($Z_{\text{chip}} = R_{\text{chip}} + jX_{\text{chip}} = 20.83 - j181.39\,\Omega$) at 866.5 MHz, i.e., the center frequency of the European UHF RFID band. The Monza X-2K is an UHF RFID Gen2 IC with 2176 bits of password-protected

Table 1. Capabilities of the sensor-augmented RFID tag.

Microcontroller	
Type	TI MSP430F5310
Program memory (kB)	32
SRAM (kB)	6
Minimum operation (V)	1.8
Active current (µA/MHz)	115
Sleep current (µA/MHz)	1.9
Wakeup time (µs)	5
Non-volatile storage	
Chip	On Semiconductor I^2C CAT24C256
Size (kB)	256
RFID communication	
Protocol	EPCglobal Class-1 Generation-2
Operating frequencies	865–868 MHz (Europe)
Chip	Impinj Monza X-2K
Modulation	Backscatter
Storage (kB)	2 (user memory)
R/W sensitivity S_{chip}	-24 dBm
Active Current (µA)	25
On-board sensors	
Temperature	MSP430 integrated sensor Analog output 9-µA supply current
3-axis accelerometer	ADXL346 13-bit/axis digital output (I^2C) 23-µA supply current
Interfaces	
Expansions	Spy-Bi-Wire, I^2C, SPI, 12 10-bit ADC channels, 47 GPIO

non-volatile memory (NVM) and an I^{2}C interface. As an I^{2}C device, Monza X-2K operates as a standard EEPROM whose contents can also be accessed wirelessly via the Gen2 protocol. The antenna design takes cue from the commercial ALN-9660 RFID tag inlay which uses meander lines to achieve a very compact form factor ($7.5 \times 1.7\,\text{cm}^2$). Note that, depending on the application and the harshness of the environment, a directive patch antenna instead of an omnidirection dipole could be used to achieve higher performance (e.g., a longer read range) and platform tolerance [10–13].

A detailed overview of computation, sensing, storage, and communication capabilities of the sensor-augmented RFID tag is given in Table 1.

3. PERFORMANCE EVALUATION

The prototype of sensor-augmented RFID tag shown in Fig. 1 has been fabricated in our labs by using a photolithography process on FR4 substrate and handy soldering off-the-shelf discrete components. The RFID antenna has been patterned directly on the PCB. A small female header and solder landings expose the Spy-Bi-Wire programming interface, the I^{2}C bus, and other MCU ports for future expansions to external sensors and devices. Detailed simulations taking into account the effect of the DC metal traces have been conducted in order to maximize the performance and optimize the design of the final prototype. The achieved results are presented and discussed below.

3.1. RFID Antenna

As for the RFID antenna, three main elements define the layout: the central loop, which primarily impact on the tuning of the real part of the input impedance and prevents potential high-voltage discharge, the meander lines to reduce the antenna size, and, finally, the capacitive loads at the antenna tips, which facilitate the impedance matching. Simulations have been performed in CST MW Studio by setting the input impedance of the antenna port equal to R_{chip} and by adding a capacitive lumped element with reactance X_{chip}. In this way, the problem is led back to the design of classic antennas with real impedance. Finally, the antenna design has been optimized by setting the minimization of the reflection coefficient at the desired frequency as the fitness function and by adopting a gradient-based interpolated quasi-newton optimizer. The E-plane polar diagram in Fig. 2(a) depicts the typical dipole radiation pattern achieved for the antenna (1.9 dBi is the maximum realized gain) while the good impedance

matching around the frequency of interest ($-13\,\text{dB}$ is the reflection coefficient magnitude at $866.5\,\text{MHz}$) is highlighted in Fig. 2(b).
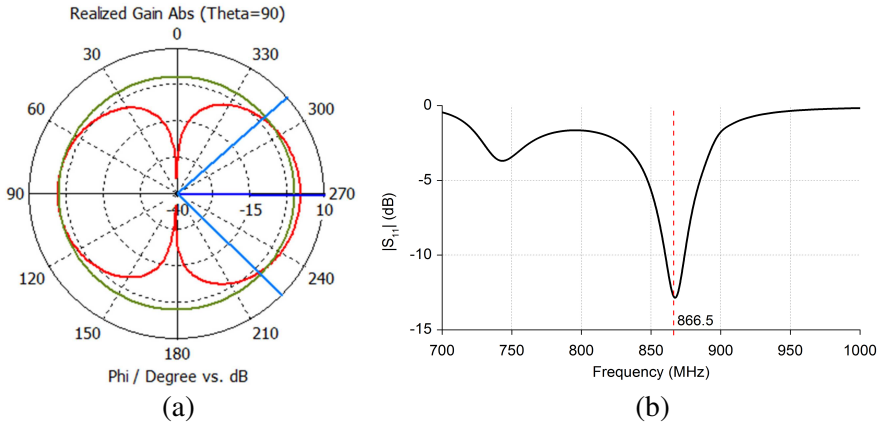

Figure 2. Simulated radiation pattern and reflection coefficient of the designed dipole-like RFID antenna. (a) E-plane polar radiation pattern. (b) Reflection coefficient.

3.2. Current Consumption and Lifetime

In order to evaluate the power consumption and, consequently, the lifetime of the the sensor-augmented RFID tag, the MCU was programmed to perform temperature and acceleration sensing, enter the sleep mode upon task completion, and be awakened periodically by an internal timer interrupt. A digital oscilloscope was used to track the voltage drop across a 1-kΩ precision shunt resistor, specifically designed for current-sensing applications, connected in series with the sensor-augmented RFID tag. Then, the DC current flowing through the device was calculated by the Ohm's law. It was found that the MCU startup and sleep phases consume $I_{\text{startup}} = 500\,\mu\text{A}$ and $I_{\text{sleep}} = 3\,\mu\text{A}$ respectively, while peaks of $I_{\text{active}} = 150\,\mu\text{A}$ occur during the active periods of the MCU performing temperature/acceleration sensing and RFID communication. The device lifetime L due to the available on-board power can be estimated by the following equation:

$$L = \frac{C \cdot (T_{\text{active}} + T_{\text{sleep}})}{I_{\text{active}} \cdot T_{\text{active}} + I_{\text{sleep}} \cdot T_{\text{sleep}}} \tag{1}$$

where C is the battery capacity in Ampere per hour and T_{active} (T_{sleep}) is the duration of the active (sleep) period. Considering

$T_{\text{active}} = 400 \, \text{ms}$ as the measured time required by the device to complete sensing and communication tasks and $C = 225 \, \text{mAh}$ as the capacity of the on-board CR2032 lithium battery, a lifetime L of approximately 3 years can be achieved when the sensor-augmented RFID tag is configured to be awakened every $T_{\text{sleep}} = 10 \, \text{s}$.

3.3. Sensitivity and Read Range

The RFID front end of the sensor-augmented tag comprises a Monza X-2K Gen2 chip and a dipole-like antenna. In order to correctly characterize the RFID performance, chip and antenna must be taken into account jointly. Indeed, the former ($S_{\text{chip}} = -24 \, \text{dBm}$ for the Monza X-2K chip) determines the minimum RF power needed for the chip to reliably decode the reader commands while the latter plays a crucial role in terms of power transfer to the chip.

   The comprehensive sensitivity of the sensor-augmented RFID tag was measured in anechoic chamber by connecting a software-defined radio (SDR) equipment implementing the Gen2 protocol [14–16] to a circularly polarized antenna (gain $G_{\text{tx}} = 5.5 \, \text{dBi}$) placed at $d = 1 - m$ line-of-sight (LOS) distance from the device oriented in the maximum-gain direction. The minimum power $P_{\text{tx,on}}$ required to communicate with the tag attached to three different surfaces (specifically foam, wood, and concrete) was recorded in the 860–930 MHz frequency band. Then, the sensitivity S_{tag} was calculated by the following equation (see [17] and [18] for its derivation) based on the free-space Friis' propagation model:

$$S_{\text{tag}} = \text{EIRP}_{\text{on}} \left(\frac{\lambda}{4\pi d} \right)^2 \eta_{\text{plf}} \quad (\text{Watt}) \qquad (2)$$

where $\text{EIRP}_{\text{on}} = P_{\text{tx,on}} G_{\text{tx}}$ is the minimum equivalent isotropically radiated power (EIRP) required to communicate with the sensor-augmented RFID tag, λ the wavelength, and $\eta_{\text{plf}} = 0.5$ the polarization loss factor due to the circularly polarized antenna of the SDR equipment.

   As shown in Fig. 3, the good impedance matching of the designed RFID antenna around 866.5 MHz (refer to Fig. 2(b)) makes the tag sensitivity S_{tag} on foam almost identical to S_{chip} in the European UHF RFID band. The approximate 2-dB difference can be accounted for by the gain of the dipole-like RFID antenna. Moreover, the rapid degradation of S_{tag} when moving away from this frequency band replicates precisely the trend of the antenna reflection coefficient. Attaching the tag to a wooden surface detunes the RFID antenna and degrades the overall performance with $-16 \, \text{dBm}$ of peak sensitivity
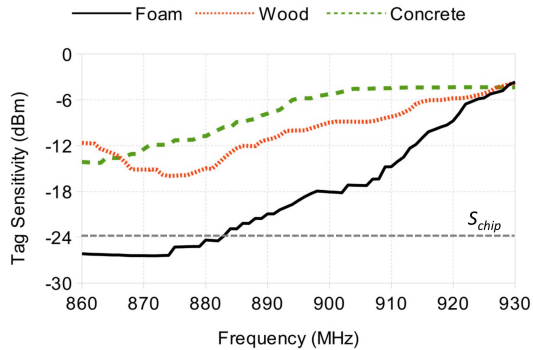
Figure 3. Measured sensitivity of the sensor-augmented RFID tag (S_{tag}) attached to different surfaces.

recorded at 886 MHz. On the other hand, concrete, while preserving the conjugate impedance matching between RFID chip and antenna around 866.5 MHz, produces slightly worse performance with -14-dBm peak sensitivity.

In order to corroborate such a result, a commercial Gen2 reader, operating in the 865–868 MHz frequency band with 3.2-W maximum EIRP according to the European regulations, was used to interrogate the sensor-augmented RFID tag at different distances. The experiments were conducted in a large lecture room with reader antenna and tag placed in LOS condition 1.5 m above the floor, both oriented in the maximum-gain direction. The reader-tag distance was increased in steps of 0.5 m and, for each measurement point, the reader was configured to perform 1000 attempts to read sensor data from the Monza X-2K user memory. The fraction of successful accesses to memory when varying the reader-tag distance is plotted in Fig. 4 for different backing materials. As shown, the success ratio for the tag attached to foam remains above 80% up to 22 m before falling sharply to zero. The small fluctuations can be accounted for by the effect of multipath. The maximum operating ranges decrease to 6 m and 5 m when the sensor-augmented RFID tag is backed by concrete and wood respectively.

3.4. Sensing Capabilities

As a simple proof of concept, the sensing capabilities of the developed RFID tag were assessed by emulating a typical application scenario concerning temperature and acceleration monitoring during parcel
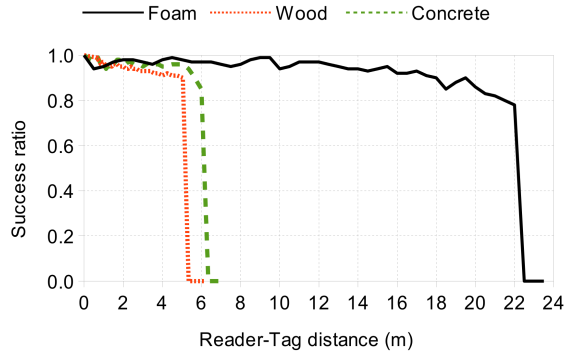
Figure 4. Measured fraction of successful reads from the user memory of the sensor-augmented RFID tag (attached to different surfaces) when varying the distance from the interrogating Gen2 reader.
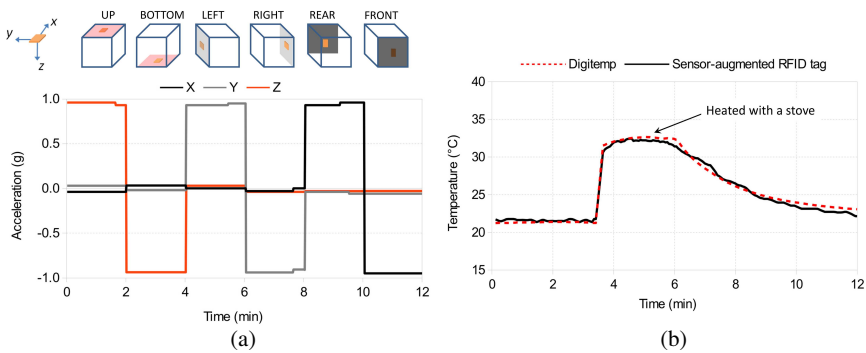

Figure 5. Acceleration and temperature logs provided by the sensor-augmented RFID tag during an emulated parcel transportation. (a) Static acceleration. (b) Temperature.

transportation.

The sensor-augmented RFID tag was attached to an internal face of a parcel containing different types of perishable goods and placed at 5 m of distance from the Gen2 reader. The device was configured to perform temperature and acceleration sensing every 10 seconds. The orientation of the parcel with respect to the ground was periodically changed (approximately every 2 minutes) so as to emulate abusive handling during the transportation. Moreover, roughly 3 minutes after the beginning of the experiment the temperature in proximity of the parcel was increased by means of a stove.

As shown in Fig. 5(a), the sensor-augmented RFID tag is able

to detect orientation changes by measuring the effect of gravity on the accelerometer axes for all the six positions experienced during the test. Furthermore, the temperature profile in Fig. 5(b) is in nearly perfect agreement with that provided by a commercial DigiTemp probe used as reference (the maximum error recorded was 1.3°C).

4. CONCLUSION

In this paper, the design, prototyping, and experimental validation of a sensor-augmented RFID tag, fully compliant with the UHF RFID Gen2 standard, have been presented. The device operates in a battery-assisted passive mode and features an ultra-low-power microcontroller, analog temperature sensor, digital 3-axis accelerometer, and a large EEPROM. The sensor readings are organized into the password-protected user memory of a new-generation I^2C-RFID chip and delivered to the interrogating reader via the zero-power backscattering technique.

A prototype of sensor-augmented RFID tag, fabricated on a PCB using low-cost off-the-shelf discrete components, has shown appealing performance in terms of sensitivity, communication range, lifetime, and sensing capabilities. More specifically, RFID-based sensor data transmissions up to approximately 22 m of distance from the interrogator have been achieved in an indoor scenario when the device in attached to foam. Instead, ranges up to 5 m and 6 m have been recorded for the device backed by wood and concrete respectively. Besides, the ultra-low power consumption of the device provides up to 3 years of lifetime when temperature and acceleration measurements are performed every 10 seconds. Finally, results from experiments emulating the transportation of a parcel containing perishable goods have demonstrated the ability of the sensor-augmented RFID tag to catch significant events such as displacements, abusive handling, and temperature threshold violations.

The proposed sensor-augmented RFID tag implementation as a PCB design using commercial off-the-shelf (COTS) components has a number of drawbacks, however, compared to an IC implementation, mainly in terms of cost and power consumption. In the progress of our research, we are planning to apply our knowledge and experience from this preliminary project to a system-on-chip solution of the sensor-augmented RFID tag.

REFERENCES

1. Mainetti, L., L. Patrono, and R. Vergallo, "IDA-pay: A secure and efficient micro-payment system based on peer-to-peer NFC technology for android mobile devices," *Journal of Communications Software and Systems*, Vol. 8, No. 4, 117–125, 2012.

2. Guido, A. L., L. Mainetti, and L. Patrono, "Evaluating potential benefits of the use of RFID, EPCglobal, and ebXML in the pharmaceutical supply chain," *International Journal of Healthcare Technology and Management*, Vol. 13, No. 4, 198–222, 2012.

3. Sample, A. P., D. J. Yeager, P. S. Powledge, A. V. Mamishev, and J. R. Smith, "Design of an RFID-based battery-free programmable sensing platform," *IEEE Transactions on Instrumentation and Measurement*, Vol. 57, No. 11, 2608–2615, Nov. 2008.

4. De Donno, D., L. Catarinucci, and L. Tarricone, "Enabling self-powered autonomous wireless sensors with new-generation I^{2}C-RFID chips," *2013 IEEE MTT-S International Microwave Symposium Digest*, 1–4, Jun. 2013.

5. Unander, T., J. Siden, and H. E. Nilsson, "Designing of RFID-based sensor solution for packaging surveillance applications," *IEEE Sensors Journal*, Vol. 11, No. 11, 3009–3018, Nov. 2011.

6. Li, T. H., A. Borisenko, and M. Bolic, "Open platform semi-passive RFID tag," *Ad-hoc, Mobile, and Wireless Networks*, Lecture Notes in Computer Sciences (LNCS), Vol. 7363, 249–259, 2012.

7. Capone, A., M. Cesana, D. De Donno, and I. Filippini, "Optimal placement of multiple interconnected gateways in heterogeneous wireless sensor networks," *NETWORKING 2009*, Lecture Notes in Computer Science (LNCS), Vol. 5550, 442–455, 2009.

8. De Donno, D., L. Catarinucci, and L. Tarricone, "An UHF RFID energy-harvesting system enhanced by a DC-DC charge pump in silicon-on-insulator technology," *IEEE Microwave and Wireless Components Letters*, Vol. 23, No. 6, 315–317, Jun. 2013.

9. Monti, G., F. Congedo, D. De Donno, and L. Tarricone, "Monopole-based rectenna for microwave energy harvesting of UHF RFID systems," *Progress In Electromagnetics Research C*, Vol. 31, 109–121, 2012.

10. Catarinucci, L., S. Tedesco, D. De Donno, and L. Tarricone, "Platform-robust passive UHF RFID tags: A case-study in robotics," *Progress In Electromagnetics Research C*, Vol. 30, 27–39, 2012.

11. Lee, H., S. Kim, D. De Donno, and M. M. Tentzeris, "A novel 'Universal' inkjet-printed EBG-backed flexible RFID for rugged on-body and metal mounted applications," *2012 IEEE MTT-S International Microwave Symposium Digest*, 1–3, Montreal, QC, Canada, 2012.

12. Liu, Y., K.-M. Luk, and H.-C. Yin, "A RFID tag metal antenna on a compact HIS substrate," *Progress In Electromagnetics Research Letters*, Vol. 18, 51–59, 2010.

13. Paredes, F., G. Zamora, S. Zuffanelli, F. J. Herraiz-Martinez, F. Martin, and J. Bonache, "Free-space and on-metal dual-band tag for UHF-RFID applications in Europe and USA," *Progress In Electromagnetics Research*, Vol. 141, 577–590, 2013.

14. De Donno, D., F. Ricciato, and L. Tarricone, "Listening to tags: Uplink RFID measurements with an open-source software-defined radio tool," *IEEE Transactions on Instrumentation and Measurement*, Vol. 62, No. 1, 109–118, Jan. 2013.

15. De Donno, D., L. Catarinucci, L. Tarricone, V. Lakafosis, and M. M. Tentzeris, "Performance enhancement of the RFID EPC Gen2 protocol by exploiting collision recovery," *Progress In Electromagnetics Research B*, Vol. 43, 53–72, 2012.

16. De Donno, D., V. Lakafosis, L. Tarricone, and M. M. Tentzeris, "Increasing performance of SDR-based collision-free RFID systems," *2012 IEEE MTT-S International Microwave Symposium Digest*, 1–3, Montreal, QC, Canada, 2012.

17. Catarinucci, L., D. De Donno, M. Guadalupi, F. Ricciato, and L. Tarricone, "Performance analysis of passive UHF RFID tags with GNU-radio," *2011 IEEE International Symposium on Antennas and Propagation (APSURSI)*, 541–544, 2011.

18. De Donno, D., L. Catarinucci, R. Colella, F. Ricciato, and L. Tarricone, "Differential RCS and sensitivity calculation of rfid tags with software-defined radio," *2012 IEEE Radio and Wireless Symposium (RWS 2012)*, 9–12, Santa Clara, CA, USA, 2012.